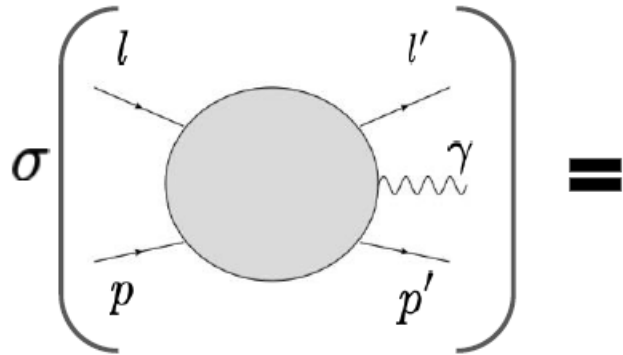


Summary on Exclusive Processes

- 1- 3D tomography of the nucleon using GPDs** by Brandom Kriesten (Virginia University)
- 2- Spin Structure of the nucleon from GPDs** by Kyle Shiells (Center for Nuclear Femtography)
- 3- Global data fits for GPDs** by Cedric Mezrag (CEA, Paris-Saclay University)
- 4- Complementary of low and high CM energy for CFFs Extraction** by François-Xavier Girod (JLab)
- 5- Complementarity of a second interaction region, Summary of the YR** by Daria Sohkan (Glasgow University)
- 6- Complementarity of a second interaction region for J/ψ and Υ production** by Sylvester Joosten (Argonne)

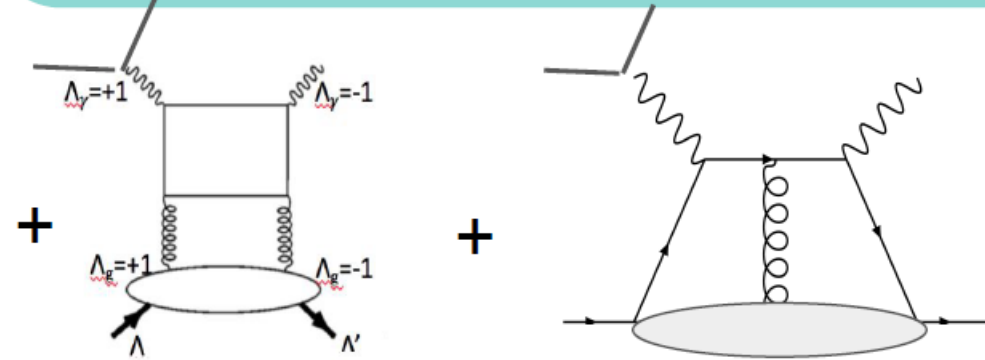
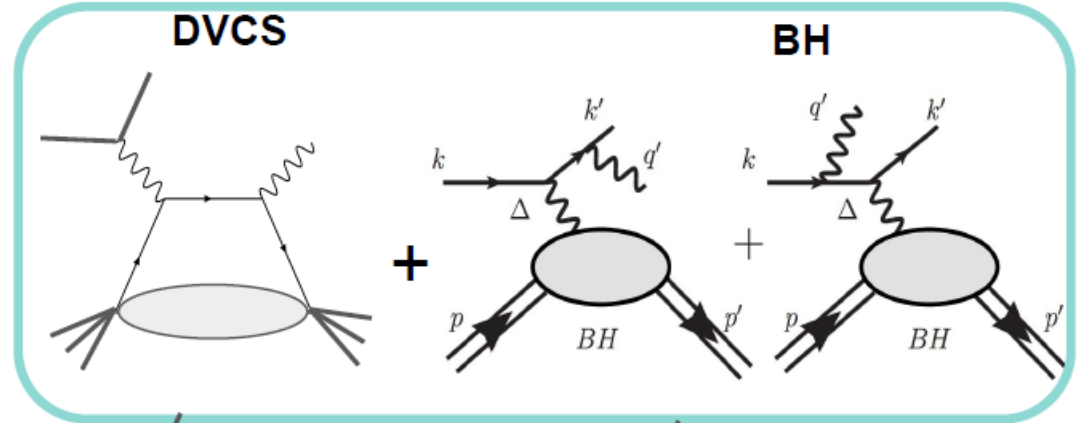
Nicole d'Hose - Xiangdong Ji
IR2@EIC, 19 March 2021

Deeply Virtual Compton Scattering



DVCS is known to probe **generalized parton distributions** and is accompanied by various background processes.

X. Ji, **PRD. 55 (1997)**



Gluon Transversity

Higher Twist

B.Kriesten, S.Liuti, et. al. **PRD. 101 (2020)**

2 major cross section analyses on the market:

2002:

Theory of deeply virtual Compton scattering on the nucleon

A.V. Belitsky^{a,b,c}, D. Müller^{c,d}, A. Kirchner^d

^aDepartment of Physics
University of Maryland at College Park
MD 20742-4111, College Park, USA

^bC.N. Yang Institute for Theoretical Physics
State University of New York at Stony Brook
NY 11794-3840, Stony Brook, USA

^cFachbereich Physik, Universität Wuppertal
D-42097 Wuppertal, Germany

^dInstitut für Theoretische Physik, Universität Regensburg
D-93040 Regensburg, Germany

- Uses finite Harmonic sums to describe angular dependence
- Twist-3 part simplified via Wandzura-Wilczek (WW) approximation

2020:

Extraction of Generalized Parton Distribution Observables from Deeply Virtual Electron Proton Scattering Experiments

Brandon Kriesten^{*}, Andrew Meyer[†], Simonetta Liuti[‡], Liliet Calero Diaz[§] and Dustin Keller[¶]

Department of Physics, University of Virginia, Charlottesville, VA 22904, USA.

Gary R. Goldstein^{**}

Department of Physics and Astronomy, Tufts University, Medford, MA 02155 USA.

J. Osvaldo Gonzalez-Hernandez^{††}

INFN, Torino
(Dated: March 5, 2020)

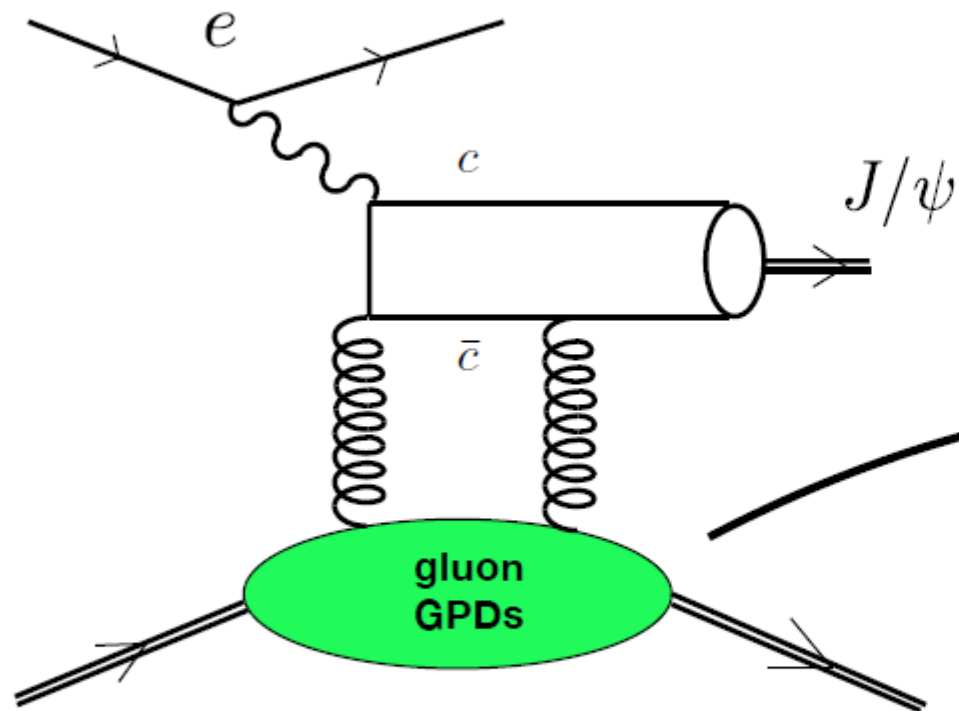
- Expresses cross sections into Rosenbluth separated form for extraction of observables
- Twist-3 GPDs kept in without approximation
- Beam and target polarization dependence is transparent

$$\frac{d^5 \sigma_{\text{unp}}^{\mathcal{I}}}{dx_{\text{Bj}} dQ^2 dt |d\phi d\phi_s} = \frac{e_l \Gamma}{|t| Q^2} \text{Re} \left\{ A_{\mathcal{I}} (F_1 \mathcal{H} + \tau F_2 \mathcal{E}) + B_{\mathcal{I}} G_M (\mathcal{H} + \mathcal{E}) + c_{\mathcal{I}} G_M \tilde{\mathcal{H}} \right. \\ \left. + \frac{K}{\sqrt{Q^2}} [A_{UU}^{(3)\mathcal{I}} (F_1 (2\tilde{\mathcal{H}}_{2T}) + \mathcal{E}_{2T} + F_2 (\mathcal{H}_{2T} + \tau \tilde{\mathcal{H}}_{2T})) + B_{UU}^{(3)\mathcal{I}} G_M \tilde{\mathcal{E}}_{2T} \right. \\ \left. + C_{UU}^{(3)\mathcal{I}} G_M (2\xi \mathcal{H}_{2T} - \tau (\tilde{\mathcal{E}}_{2T} - \xi \mathcal{E}_{2T})) \right\}$$

Twist-2 AM!

Twist-3 OAM!!

J/ψ production:



- Resolution scale: $M_{J/\psi}^2 + Q^2$ allows unprecedented access to small- x gluons

$$H_g(x), E_g(x) \quad \text{Gluon twist-2 GPDs}$$

Possibility: $L_g = J_g - \Delta G$

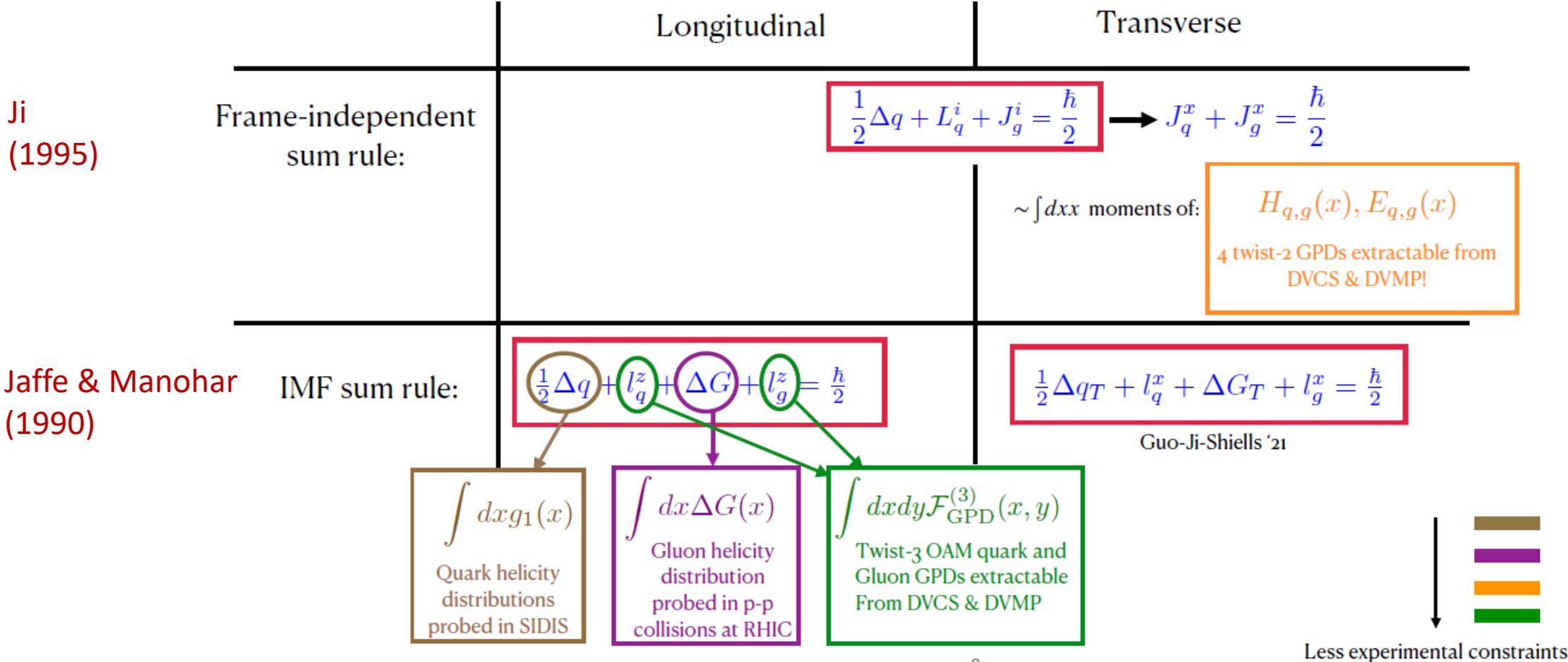
- Theory description more challenging than DVCS, multiple approaches proposed

e.g. 2 Gluon form factors: Frankfurt, Strikman (2002)

EIC:

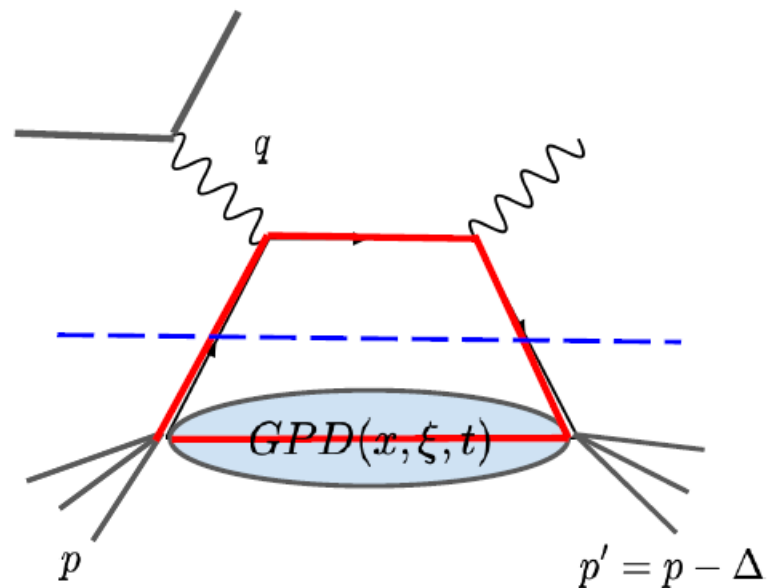
High CM energy $\sqrt{s} \sim 173$ GeV allows much broader (x, Q^2) coverage, especially low x

Experimental testing:



- priorities
- **1st order:** reduce uncertainty of Spin PDFs $g_1(x, Q^2)$ and $\Delta G(x, Q^2)$
 - **2nd order:** measure twist-2 GPDs H & E for quark and gluon $\xrightarrow{\text{Completes}} J_q + J_g = \frac{\hbar}{2}$
 - **3rd order:** measure the twist-3 GPDs of AM $\xrightarrow{\text{Completes}} \frac{1}{2}\Delta q + l_q^z + \Delta G + l_g^z = \frac{\hbar}{2}$

Issues with GPDs: they come convoluted with Wilson coefficient functions (Compton Form Factors) meaning we only have experimental access to [integrals \(ReCFF\)](#) or [specific points in \$x\$ \(ImCFF\)](#) of these distributions.



$$\int_{-1}^{+1} dx \frac{F^q(x, \xi, t)}{x - \xi + i\epsilon} = \mathcal{P} \int_{-1}^{+1} dx \frac{F^q(x, \xi, t)}{x - \xi} - i\pi F(\xi, \xi, t)$$

Additional Tools: Constraints from Lattice QCD

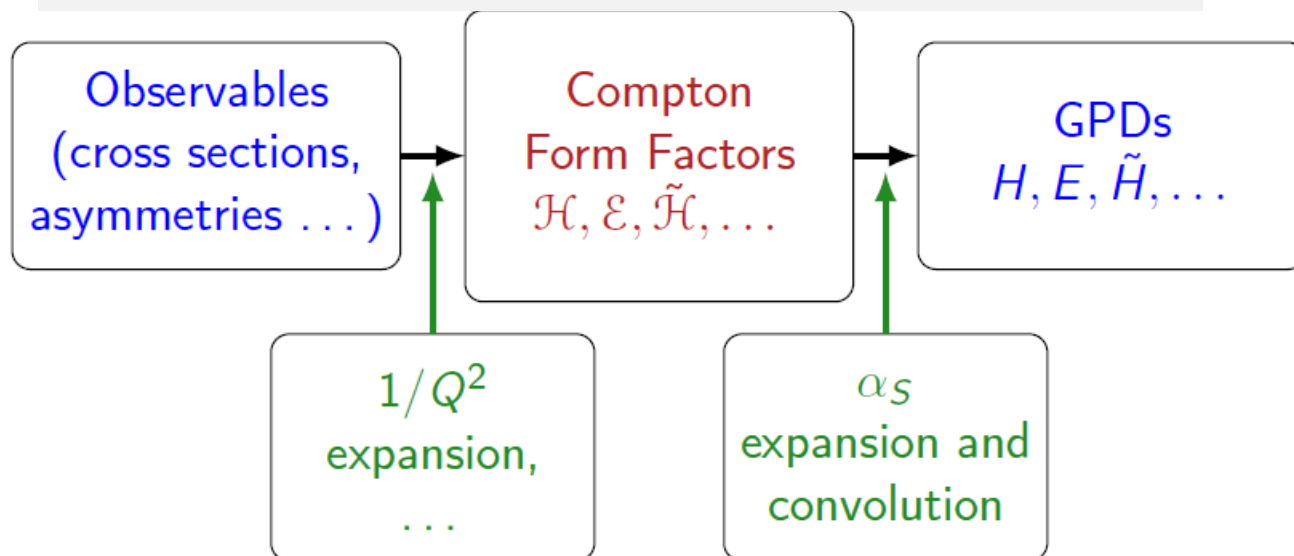
Femtography using Artificial Intelligence

GPDs at EIC: Fits, Modelling, and opportunities

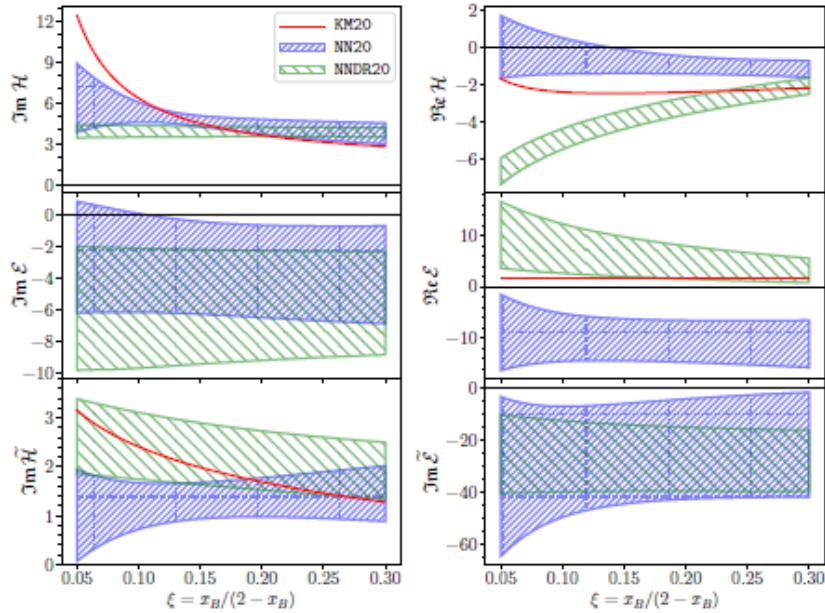
Cédric Mezrag

DPhN, Irfu, CEA, Université Paris-Saclay

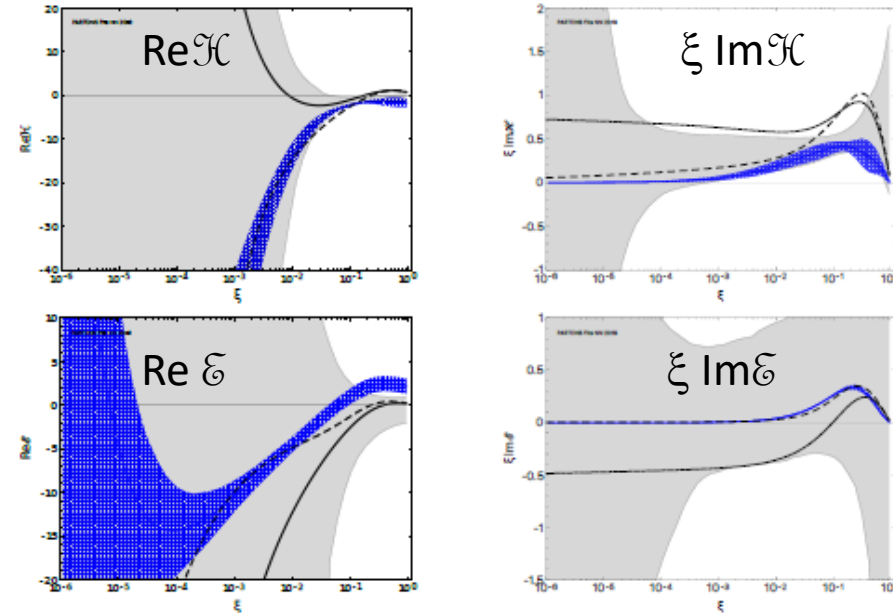
Experimental connection to GPDs



- CFFs play today a central role in our understanding of GPDs
- Extraction generally focused on CFFs



M. Cuić *et al.*, PRL 125, (2020), 232005



H. Moutarde *et al.*, EPJC 79, (2019), 614

- Recent effort on bias reduction in CFF extraction (ANN)
additional ongoing studies, J. Grigsby *et al.*, arXiv:2012.04801
- Studies of ANN architecture to fulfil GPDs properties (dispersion relation, polynomiality, ...)
- Recent efforts on propagation of uncertainties (allowing impact studies for EIC and EICC)

$$\mathcal{H}(\xi, t, Q^2) = \int_{-1}^1 \frac{dx}{\xi} C \left(\frac{x}{\xi}, \frac{Q^2}{\mu^2}, \alpha_s(\mu) \right) H(x, \xi, t, \mu)$$

Definition of the problem

Being given \mathcal{H} on a large kinematical range and with excellent precision, is it possible to recover H unambiguously?

- Not a new problem (already raised in the 1990s), but it remains open, generally speaking.
- At LO, the answer is definitely no. We can find 0-order shadow GPDs h_0 providing that
 - ▶ $h_0(x, 0, 0) = 0$ and $h_0(x, x, t) = 0$
 - ▶ h_0 has no D-term.

Role of higher orders corrections and evolution equations?

PARTONS

partons.cea.fr



B. Berthou *et al.*, EPJC 78 (2018) 478

Gepard

calculon.phy.hr/gpd/server/index.html



K. Kumericki, EPJ Web Conf. 112 (2016) 01012

- Similarities : NLO computations, BM formalism, ANN, ...
- Differences : models, evolution, dissemination, ...

Physics impact

These integrated softwares are the mandatory path toward reliable multichannel analyses.

Complementary of low and high CM energy for CFFs Extraction

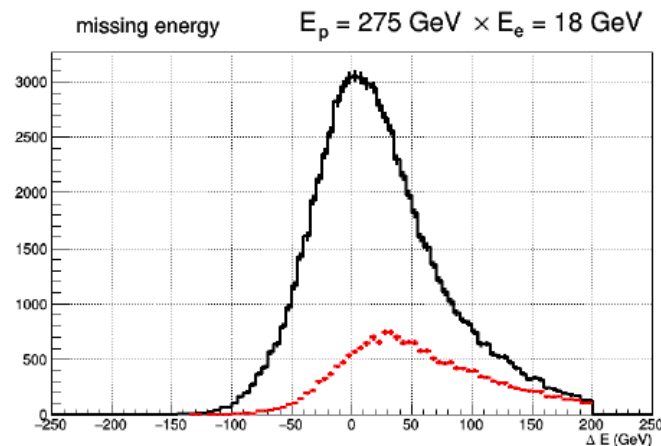
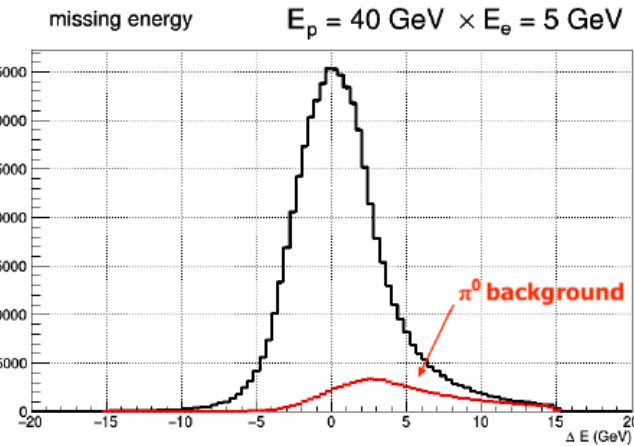
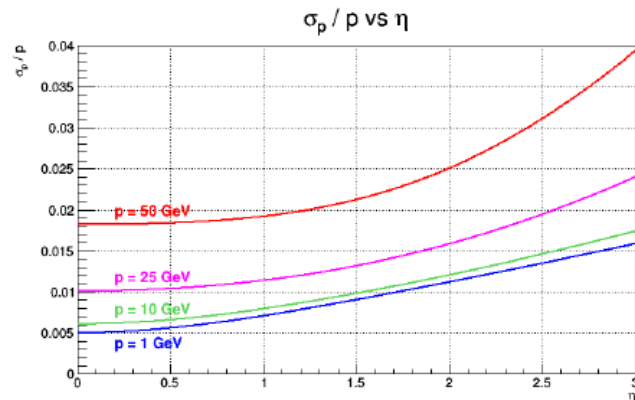
EIC Si Tracker Concept

François-Xavier Girod

Si tracker concept
Resolutions comparable to EIC Handbook v1

Detect all final particles $ep \rightarrow ep\gamma$
Apply energy momentum conservation cuts

Background from π^0 decay depends on EM granularity



Local fits of observable set in bins

Integrated luminosity

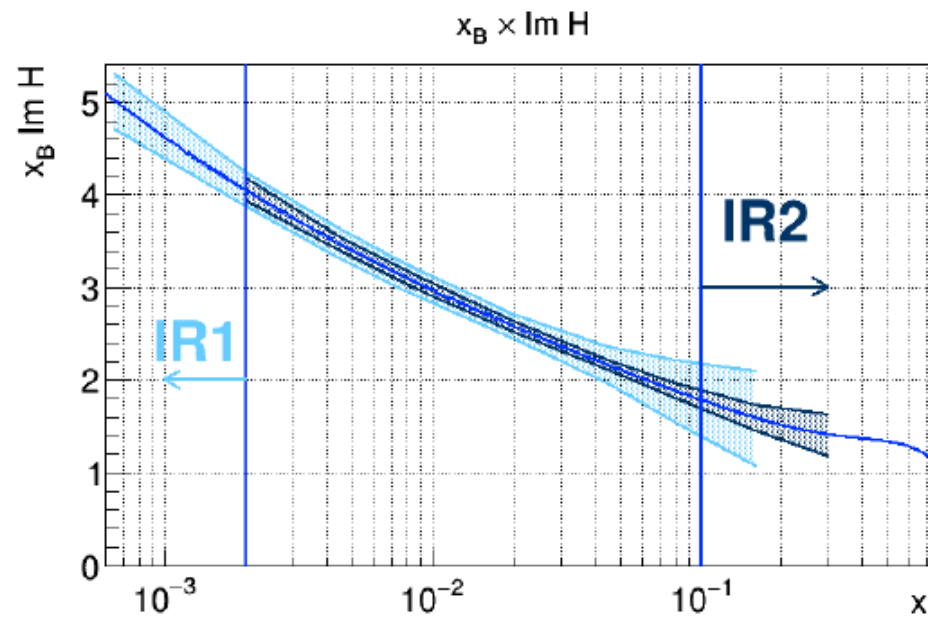
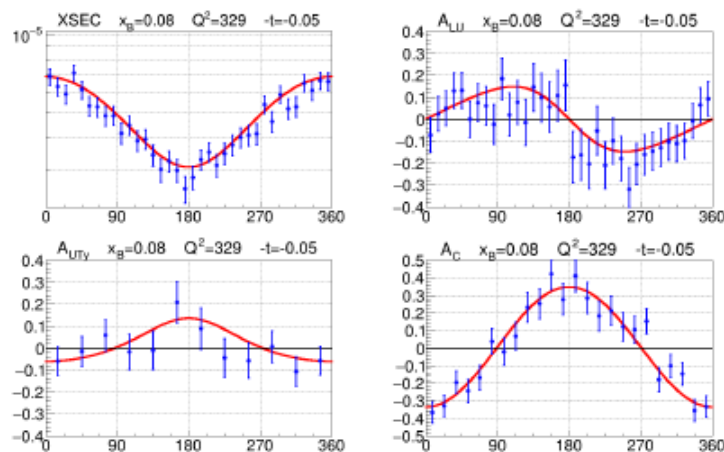
~ one continuous year at $10^{34} \text{cm}^{-2} \text{s}^{-1}$

Includes 3% systematics on

polarizations and 5% on absolute

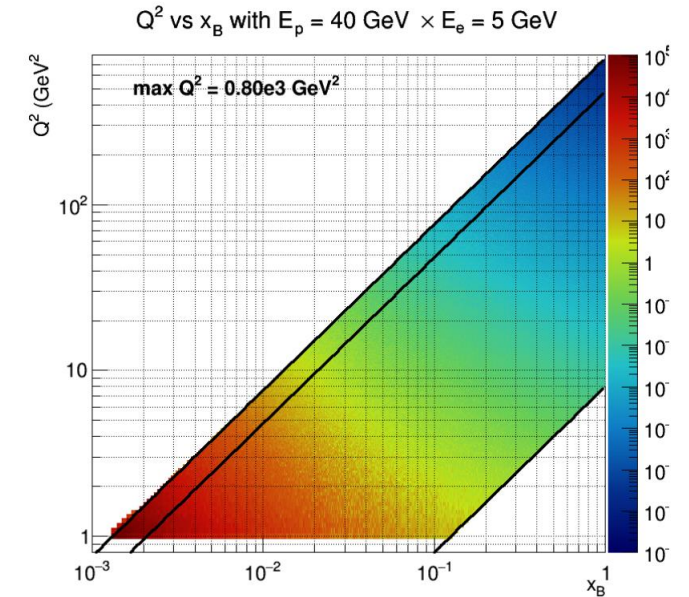
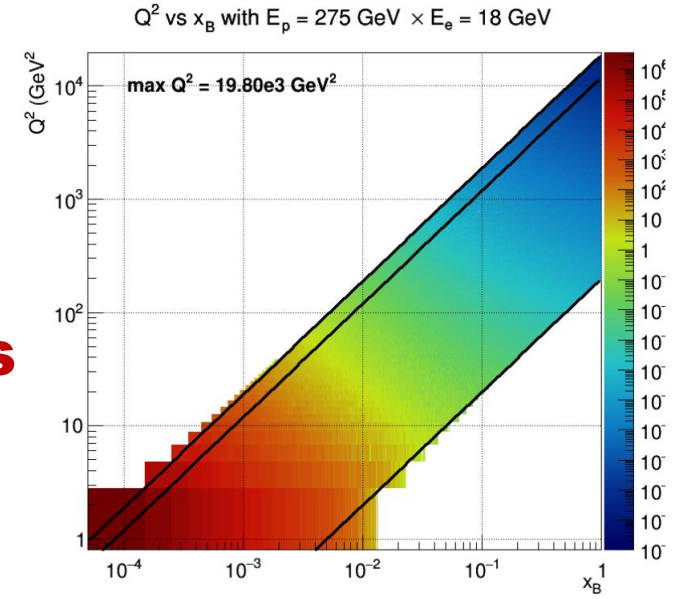
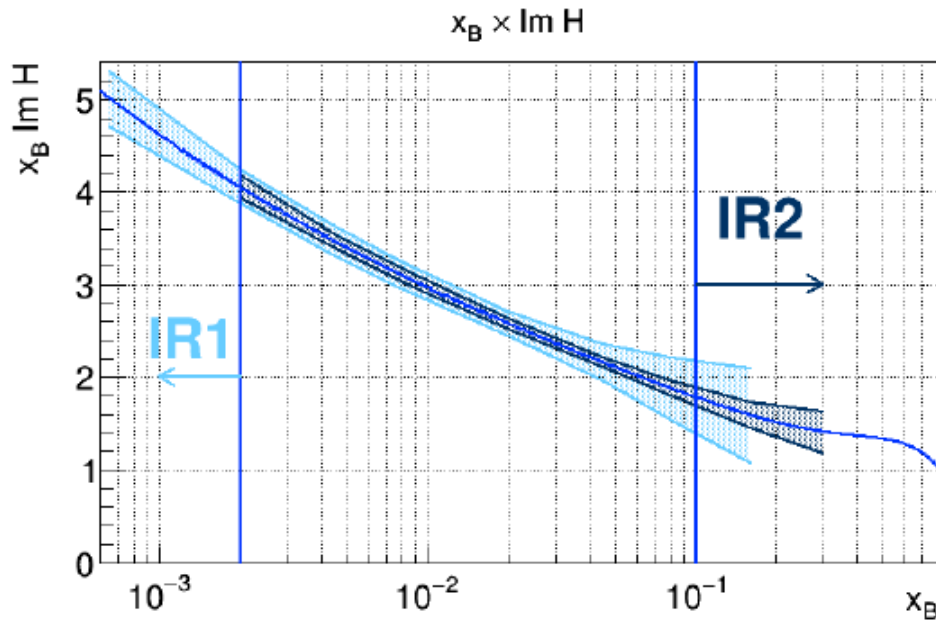
normalization \otimes acceptance \otimes efficiency

	$\int \mathcal{L}$	$A_{e,p}$			
unpolarized	200 fb^{-1}	σ	A_{LU}		
L polarized	100 fb^{-1}	A_{UL}	A_{LL}		
T polarized	100 fb^{-1}	A_{UTx}	A_{UTy}	A_{LTx}	A_{LTy}
e^+	100 fb^{-1}	A^C	A_{LU}^C		



Complementarity of IR1 and IR2

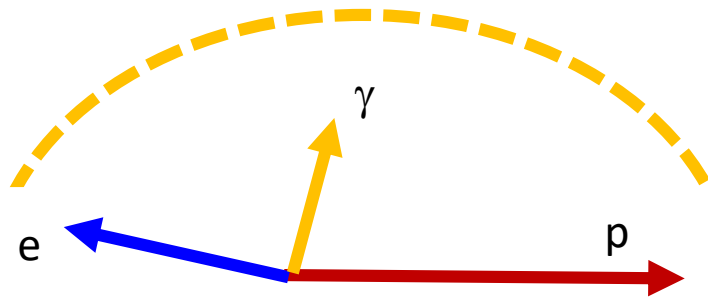
Complementarity of low and high CM energies



Exclusive reactions

$e p \rightarrow e p \gamma$ DVCS $\gamma p \rightarrow p \ell^+ \ell^-$ TCS
 $e p \rightarrow e p \pi^0$
 $e p \rightarrow e p J/\psi$ & with quasi-real photons
 $e p \rightarrow e p Y(1S)$ & with quasi-real photons

Exclusive reactions on light nuclei



E_e (GeV)	E_p (GeV)	\sqrt{s} (GeV)
5	41	29
5	100	45
10	100	63
18	275	141

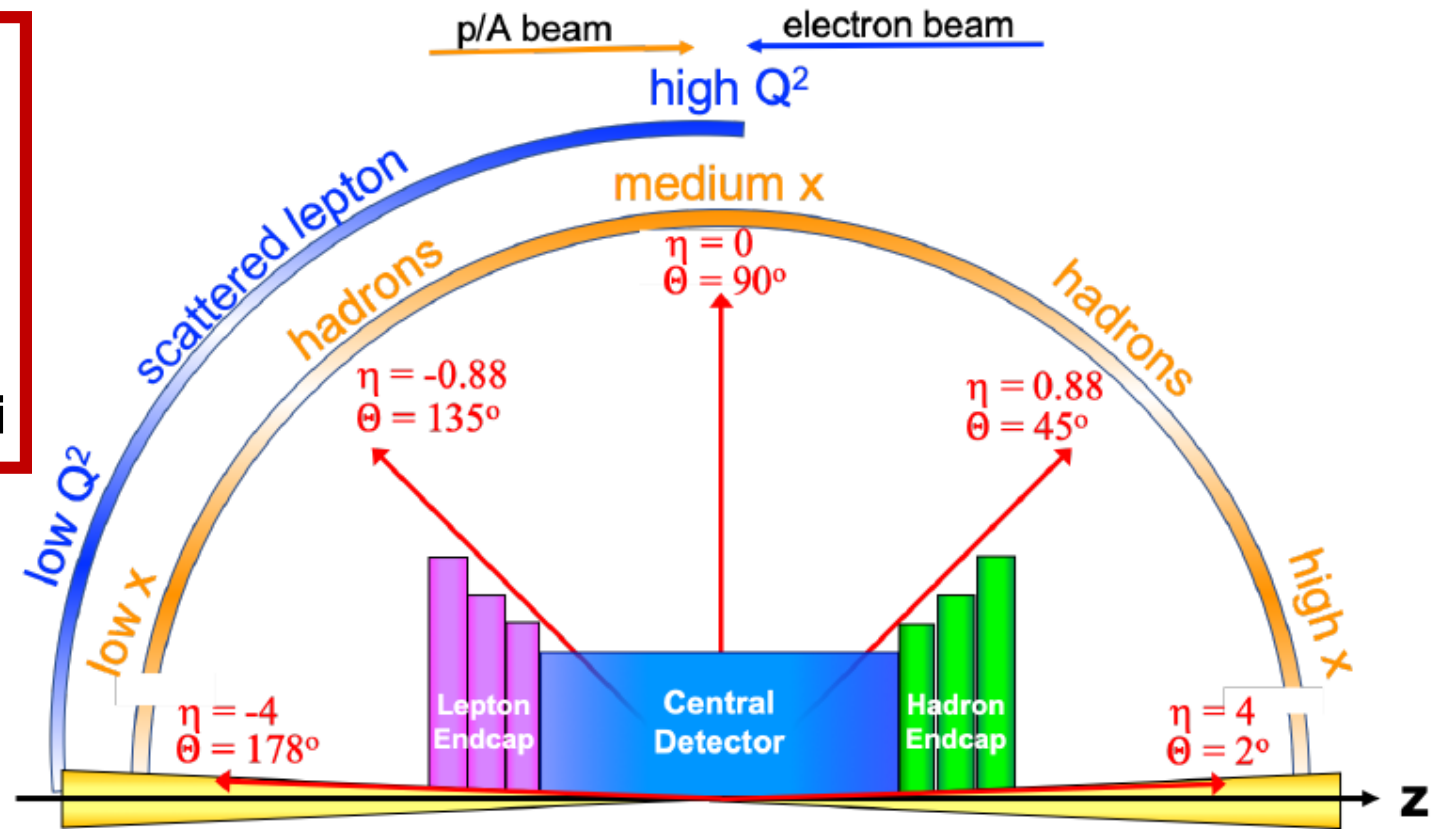


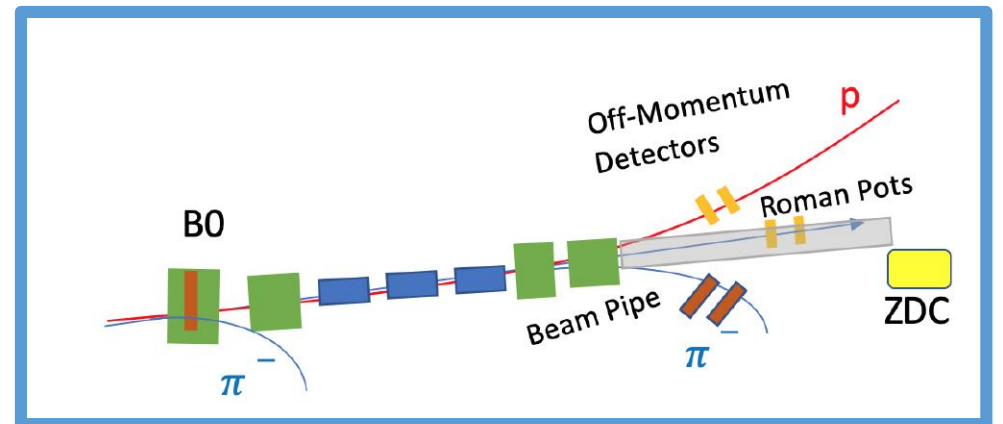
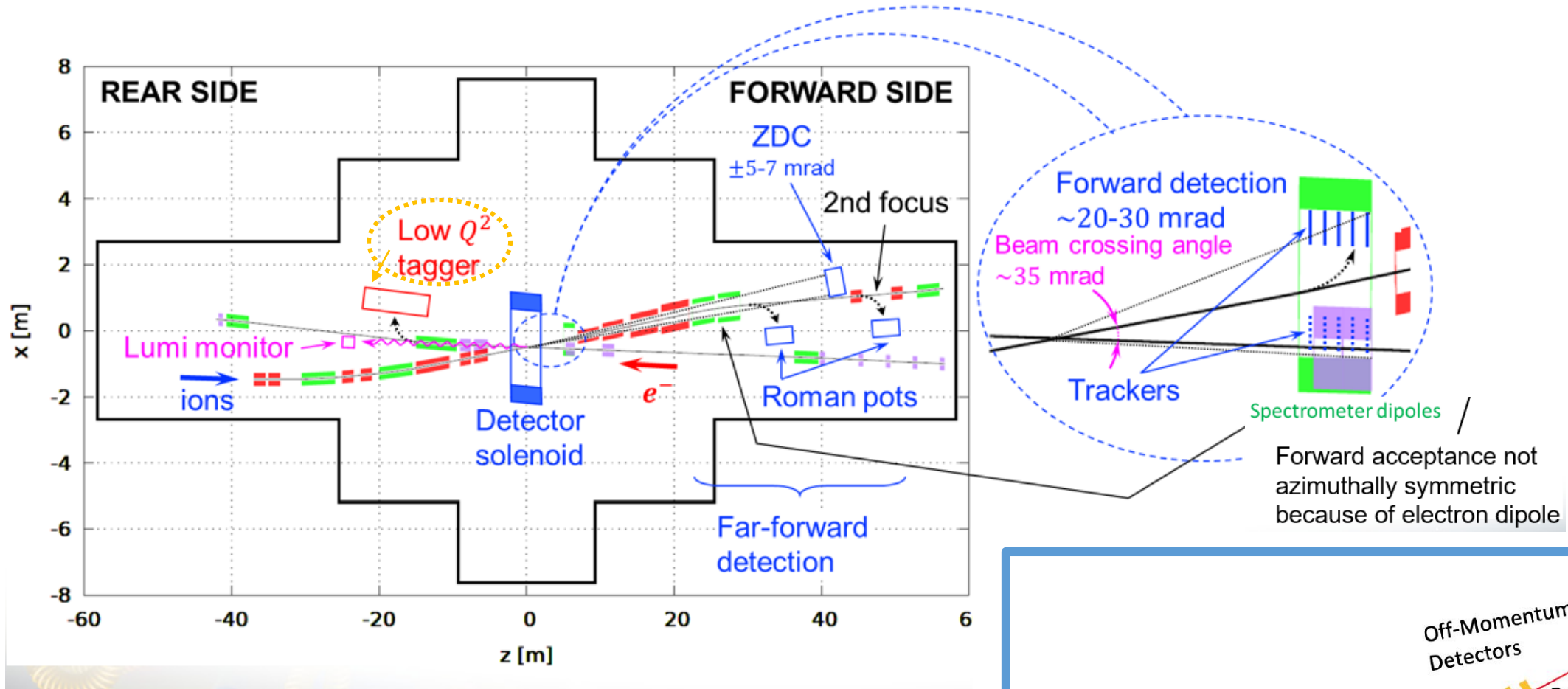
Figure 2.2: Schematic showing the distribution of the scattered lepton and hadrons for different $x - Q^2$ regions over the detector polar angle / pseudorapidity coverage.

When $\sqrt{s} \nearrow$ the outgoing particles are more focused on the beam axis

The Protons have always to be detected in the very forward direction

2nd IR Schematic

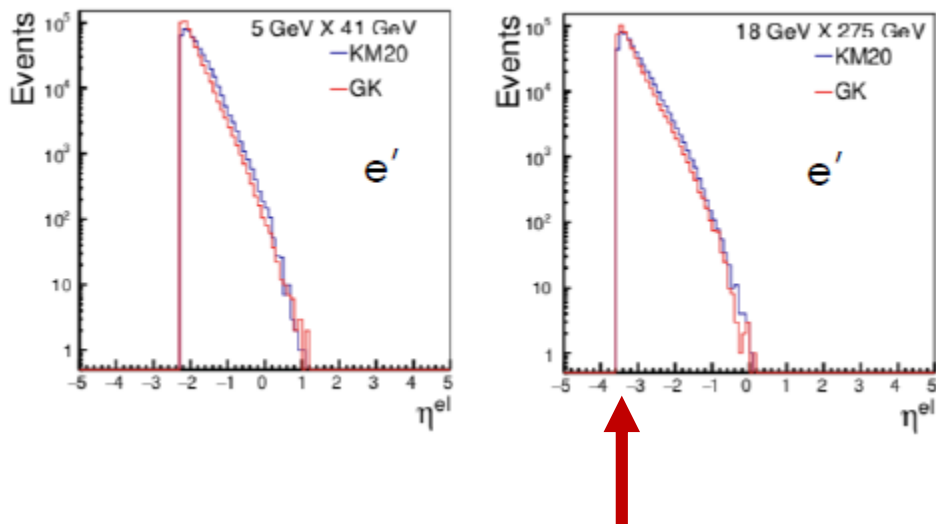
Vasiliy Morozov
on behalf of 2nd IR Design Team



DVCS and π^0 production

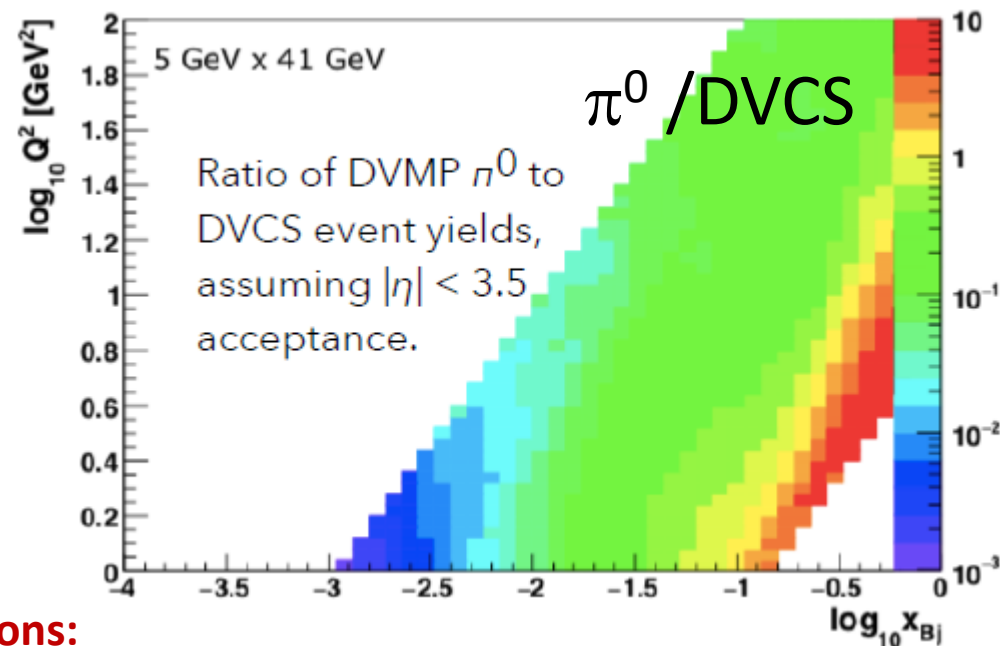
DVCS and π^0 generated with Goloskokov-Kroll (GK, red) and Kumerički-Mueller (KM, blue) models.

Scattered Electrons:



Nominal central detector acceptance ($|\eta| < 3.5$):
loss of 14% of DVCS events, 11% of π^0 events,
at the lowest x_B for highest collision energy.

Additional effect of photon acceptance places
 total loss at **17% of DVCS, 12% of π^0 events** at
highest collision energy.



Photons:

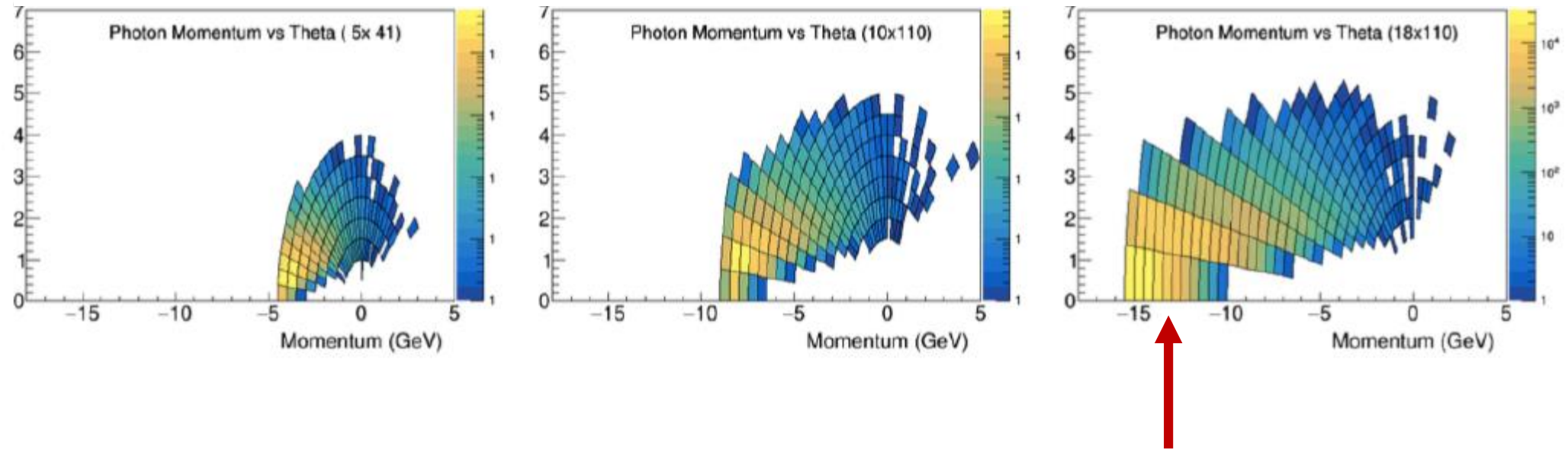
Contamination of π^0 decay photons in DVCS reconstruction **poses the biggest problem at lowest CM energies and at high x_B .**

Can be mitigated by EMCal with high granularity (π^0 photon opening angle peaks at ~ 1.5 deg) in the forward direction.

For π^0 reconstruction, also need EMCal energy threshold as low as possible.

Coherent DVCS on ^4He

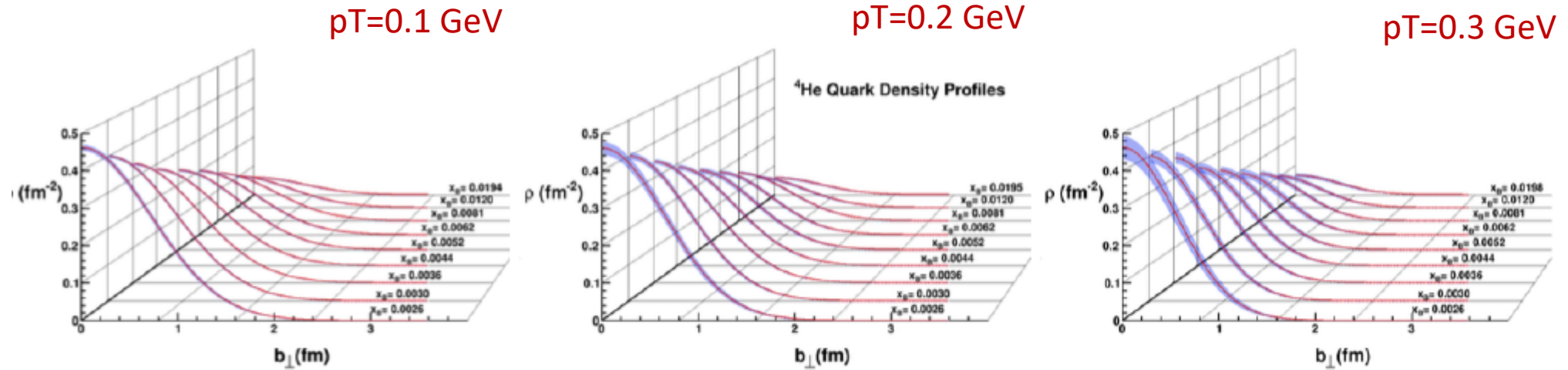
Simulated with the TOPEG generator, ^4He the most challenging case (out of light ions) for detectors:



Scatt Electron: Nominal central detector acceptance cuts into the lowest-angle electrons and photons, worst at highest beam energies (**loss of ~20%**): **cuts out lowest- x_B** .

Recoil: **Detection of recoil critical:** at low x_B , t_{min} is below **detector acceptance (Roman Pots)**, while max $|t|$ is limited by **luminosity**.

Min transverse momentum detectable: 0.2 GeV/c, corresponds to $-t \sim 0.04 \text{ GeV}^2$.

Coherent DVCS on ${}^4\text{He}$ Impact of p_T threshold for the recoil detection

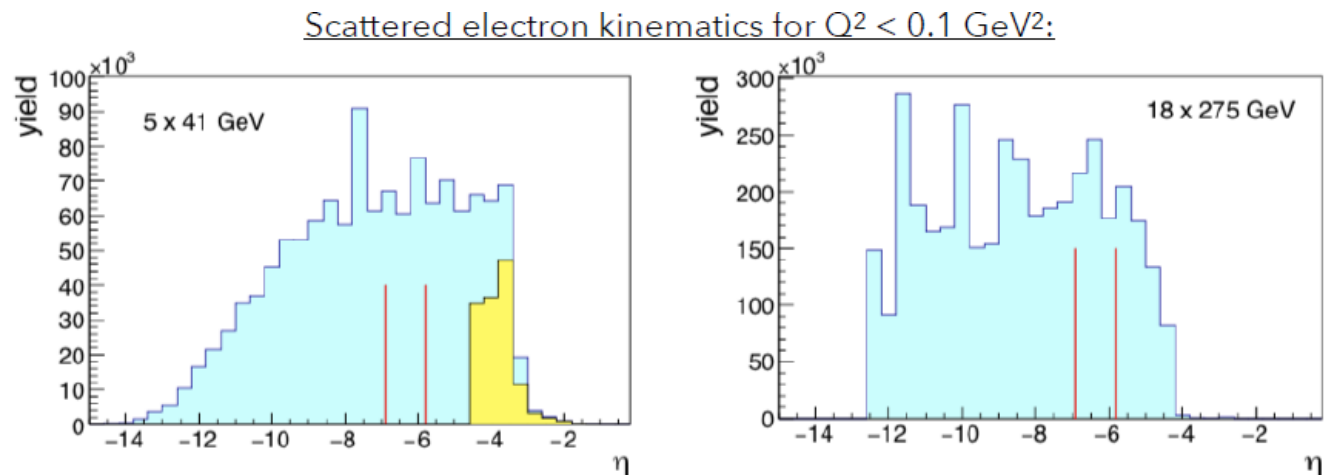
Quark density profiles for coherent DVCS off ${}^4\text{He}$ generated with TOPEG. Extraction based on fit using leading-order formalism and three Roman Pot p_T thresholds: 0.1 (left), 0.2 (centre) and 0.3 GeV (right).

Minimum reach in $-t$ directly affects the uncertainties on the density profiles.

Time-like Compton Scattering

Quasi-real photoproduction: $Q^2 < 0.1 \text{ GeV}^2$. Generated with toy MC using GK model.

Scattered electron



Turquoise: all generated, yellow: all particles reconstructed, central detector acceptance $|\eta| < 4.5$. Red lines: proposed low- Q^2 tagger acceptance ($-6.9 < \eta < -5.8$): does not add much.

Low- Q^2 tagger may help with suppression of background, but is not needed for calculation of t : resolution is better when t is calculated from the scattered proton.

Lepton (e or μ) pairs

Muon final-state distributions: identical to electron ones.

Advantages of **muon detector**:

- No combinatorial background with scattered electron from a high Q^2 process,
- Better Q'^2 resolution: absence of Bremsstrahlung, better signal-to-noise ratio,
- Systematic checks of e^+e^- analysis,
- Doubling of statistics.

EXCLUSIVE QUARKONIUM PRODUCTION

What do we know?

Near Threshold:

- Origin of proton mass, trace anomaly of the QCD EMT
- Gluonic Van der Waals force, possible quarkonium-nucleon/nucleus bound states
- Mechanism for quarkonium production
- Test SRC universality with a gluonic probe

Electro-Production at high energies:

- Access Gluon GPD: Full 3D tomography of the gluonic structure of the nucleon
- Matter radius of nuclei
- Sensitive to onset of saturation
- L-T Separation and Q^2 dependence of R for quarkonium production

J/ψ photo-production well-constrained at high energies

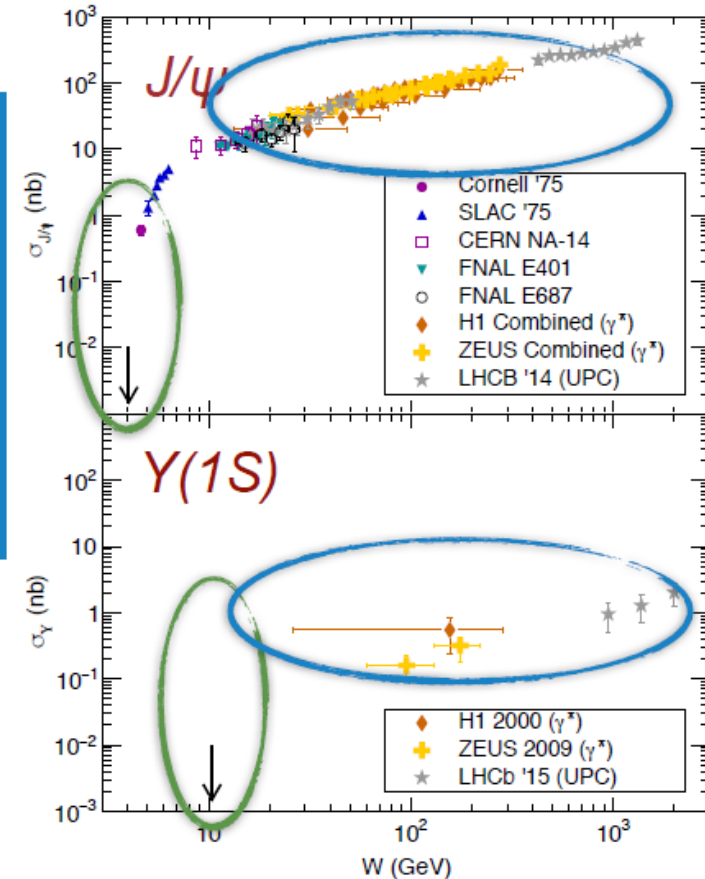
$Y(1S)$: not much available

Almost no data near threshold

Electro-production almost completely understood

J/ψ at JLab
 $Y(1s)$ at EIC

J/ψ and
 $Y(1s)$ at EIC

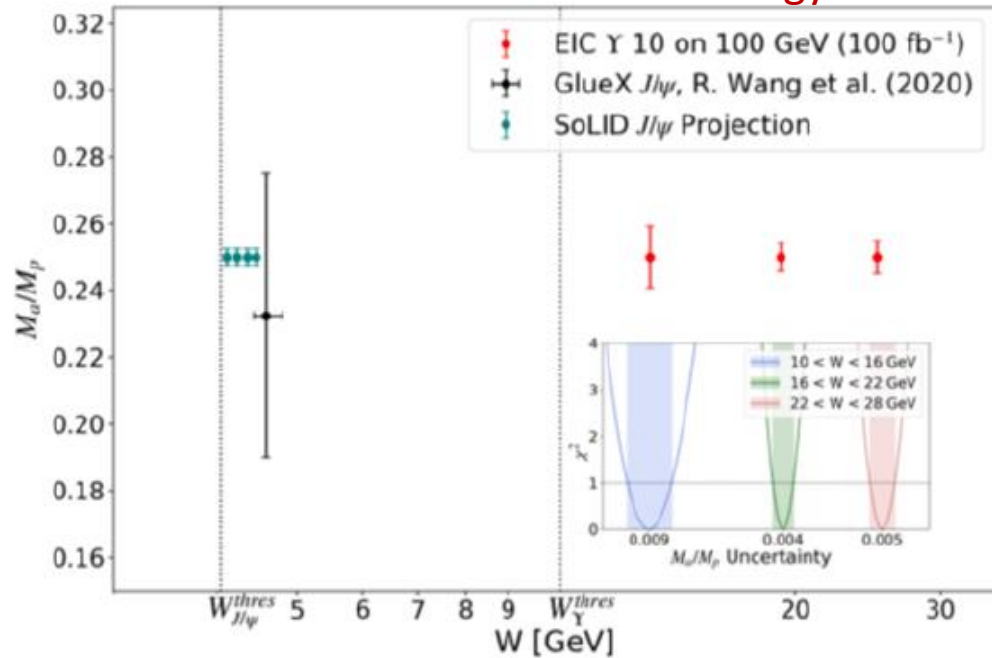


$Y(1S)$ PHOTOPRODUCTION AT EIC
...Threshold measurement possible!

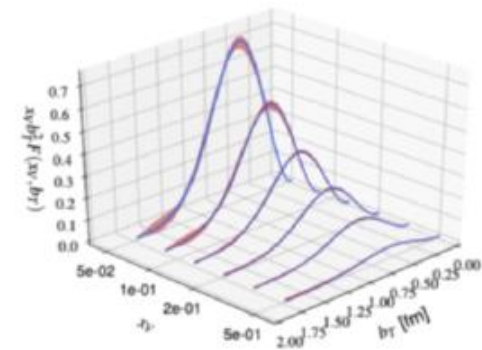
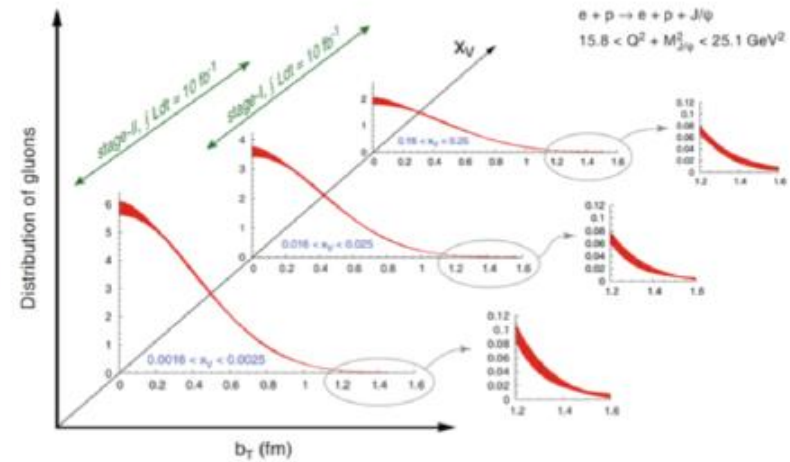
PROJECTED RESULTS FROM YELLOW REPORT

Quantum anomalous energy from Upsilon photoproduction

Medium energy is the best



3D gluon imaging from J/ψ and Υ DVMP

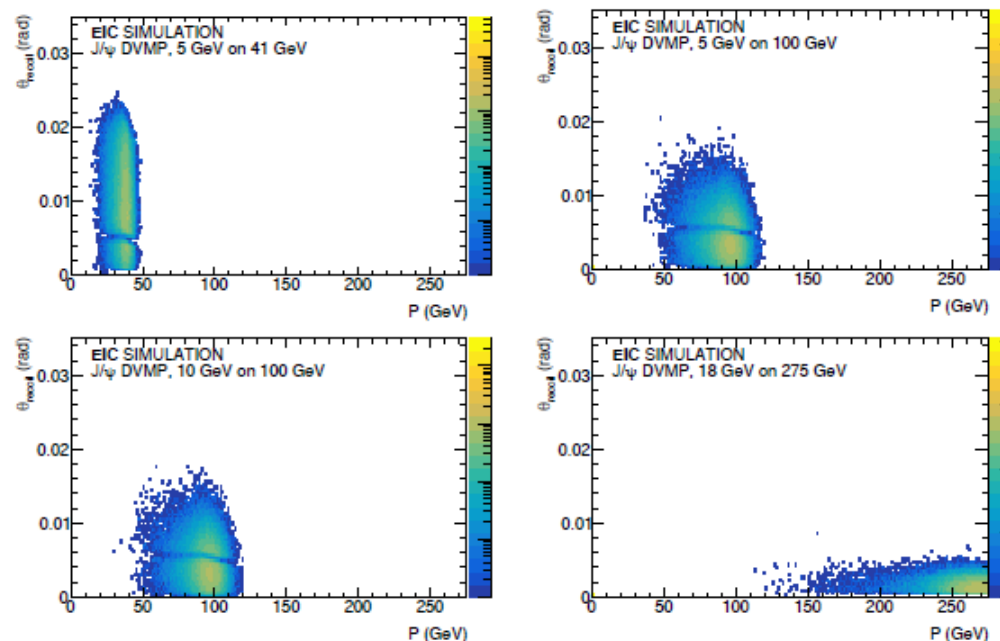
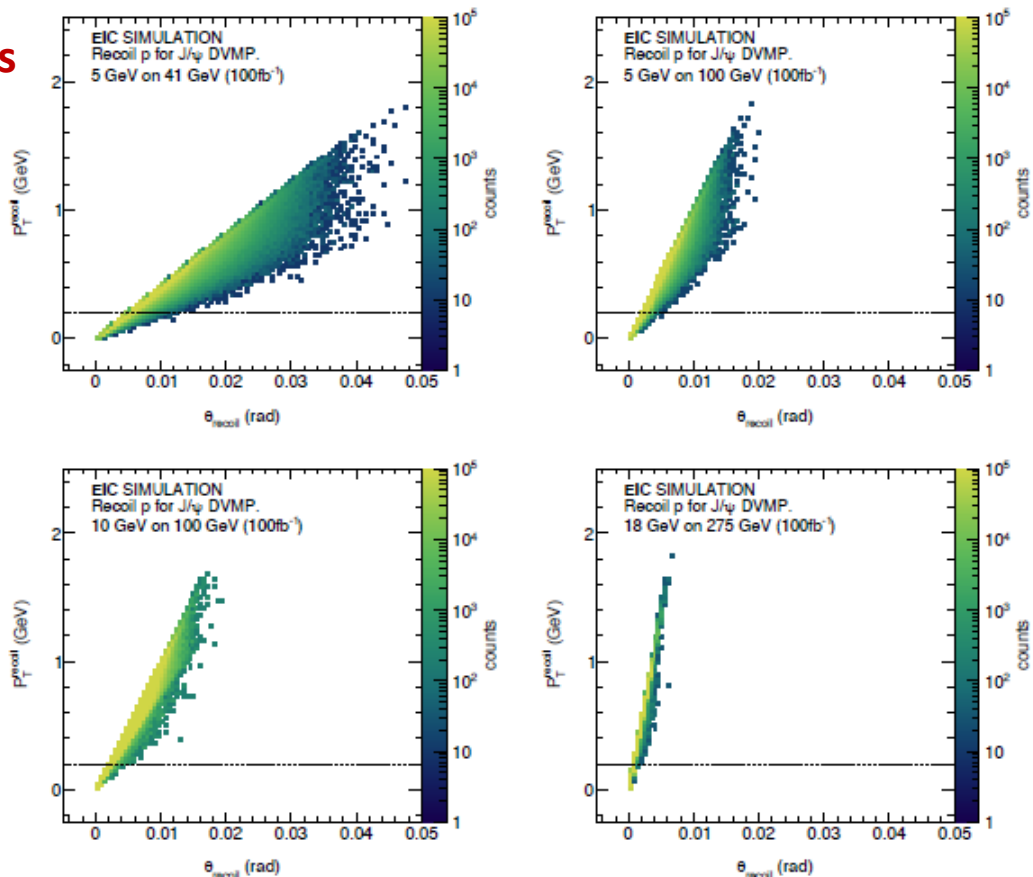


...Assuming 100fb⁻¹

RECOIL PROTONS REQUIRE FAR-FORWARD DETECTION

Need continuous far-forward detection with roman pots and B0

protons



Proposed nominal far-forward system in YR can do the job for DVMP on the proton. Lower energies depend mostly on B0

Lower p_T coverage may be important for exclusive coherent/incoherent reactions off nuclei

PHOTOPRODUCTION PERFORMANCE

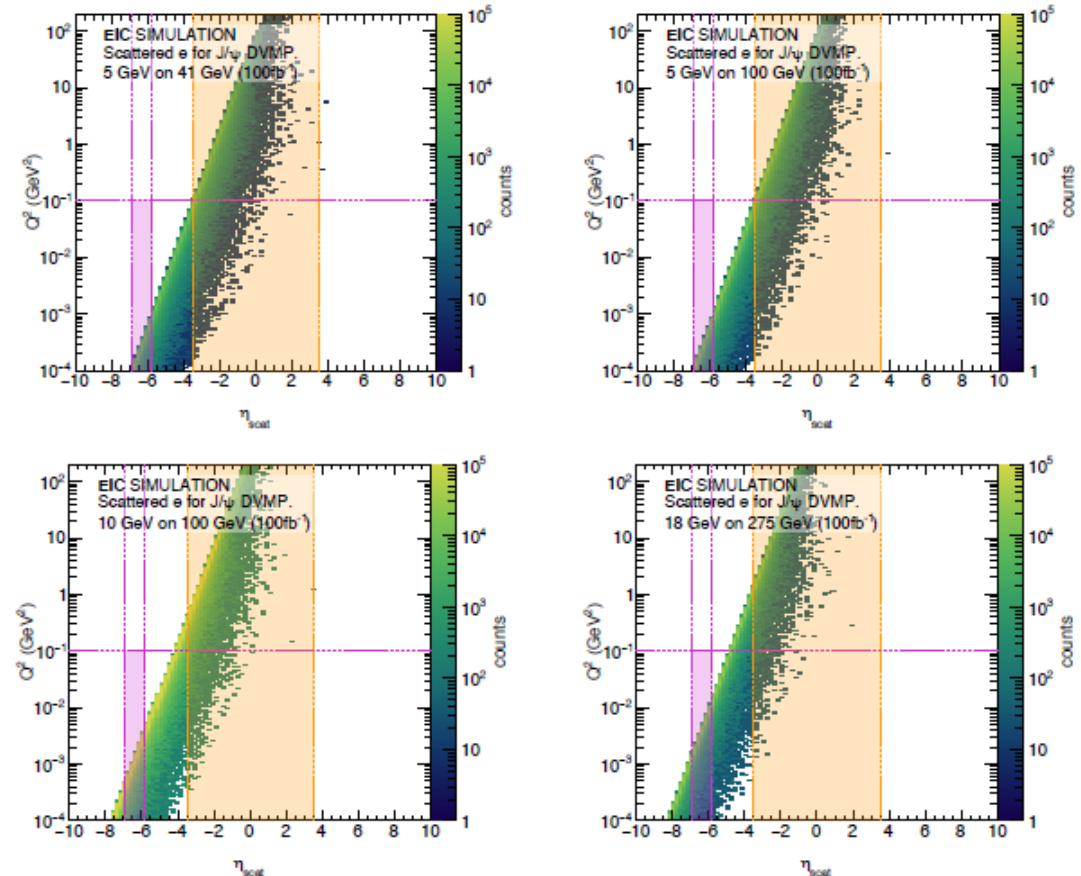
Nominal reference detector not optimized for exclusive quasi-real production

Scattered electrons:

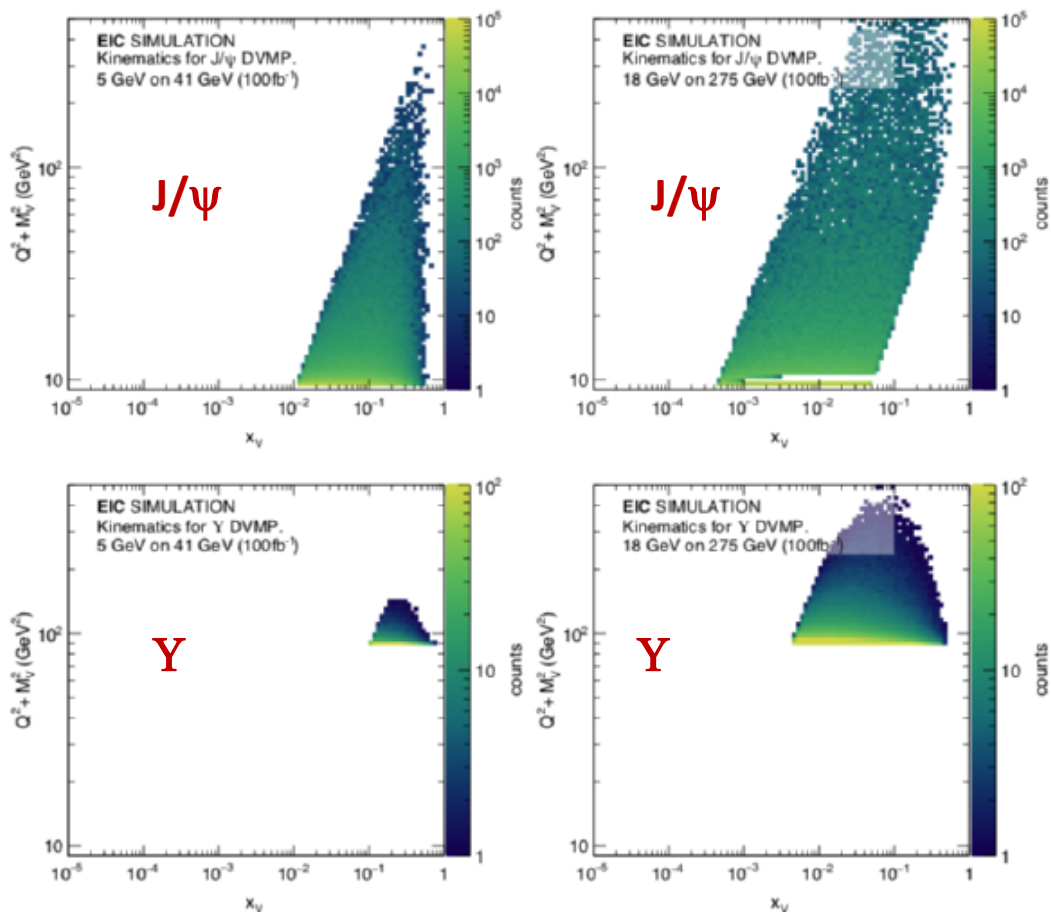
Pink: low-Q2 tagger
Orange: nominal central detector with $|\eta| < 3.5$

Extended **central detector acceptance below $\eta < -3.5$** will boost quasi real acceptance

Maybe easier, an **extended low-Q2 tagger acceptance** can dramatically increase rates



ARGUMENTS FOR A COMPLEMENTARY APPROACH



$$x_V = (Q^2 + M_V^2) / (2P \cdot q)$$

Medium-energies maximize DVMP threshold reach: higher energies restricted by resolution at low y .

To maximize photoproduction (true for all energies): Good acceptance in backward region, and good low- Q^2 tagger

Higher-energy configurations more potent for GPD imaging due to greater photon flux, larger Q^2 coverage. Note, intrinsically already at larger x (large quarkonium mass shifts kinematics to higher x)

Medium and low energy in particular need higher luminosity to get balanced statistics for entire phase space

Comprehensive DVMP program needs high luminosity at both high and medium energies: $O(100\text{fb}^{-1} \sim 110 \text{ days at } 10^{34}/\text{cm}^2/\text{s})$